Journal of Materials and Environmental Science
ISSN : 2028-2508
e-ISSN : 2737-890X
CODEN : JMESCN

J. Mater. Environ. Sci., 2023, Volume 14, Issue 11, Page 1230-1244

http://www.jmaterenvironsci.com

Modulation of the physical properties of spray-deposited cobalt selenide nanofilm via yttrium doping for photovoltaic purposes.

Nwamaka I. Akpu[a], Cissan A. Sylvanus[b], Elizabeth C. Nwaokorongwu[a]. Imosobomeh L. Ikhioya[c, f*], Emmanuel O. Okechukwu [d], Laeticia U. Ugwu [d, e], Azubuike J. Ekpunobi [d]

[a] *Department of Physics, Michael Okpara University of Agriculture, Umudike, 7267, Umuahia, Abia State, Nigeria*
[b] *Department of Industrial Physics, Abia State University, Uturu*
[c] *Department of Physics and Astronomy, University of Nigeria, Nsukka, 410001, Nigeria*
[d] *Department of Physics and Industrial Physics, Nnamdi Azikiwe University, Awka Nigeria*
[e] *Department of Physics Education, Federal College of Education (Technical) Umunze, Anambra State, Nigeria*
[f] *National Centre for Physics, Quaid-i-Azam University Campus, Islamabad, 44000, Pakistan.*
Corresponding author, Email address: imosobomeh.ikhioya@unn.edu.ng, https://orcid.org/0000-0002-5959-4427

Received *15 Sept 2023,*
Revised *15 Nov 2023,*
Accepted *18 Nov 2023*

Keywords:
- ✓ *spray pyrolysis,*
- ✓ *yttrium,*
- ✓ *cobalt selenide,*
- ✓ *dopant,*
- ✓ *absorbance,*
- ✓ *energy band gap,*

Citation*: Akpu N.I., Sylvanus C.A., Nwaokorongwu E.C., Ikhioya I.L., Okechukwu E.O., Ugwu L.U., Ekpunobi A.J. (2023) Modulation of the physical properties of spray-deposited cobalt selenide nanofilm via yttrium doping for photovoltaic purposes, J. Mater. Environ. Sci., 14(11), 1230-1244*

Abstract: The Spray pyrolysis technique was satisfactorily used to produce thin materials of undoped CoSe and yttrium doped CoSe. The purpose of this investigation was to deduce the significance of doping on the features of yttrium-doped CoSe (Y:CoSe). Undoped CoSe and Y:CoSe (0.1 – 0.4 mol%) were produced at a constant temperature of 400°C. The aftermath of yttrium incorporation on the optical, structural, composition, morphology, and electrical features of CoSe was ascertained via the utilization of a spectrophotometer (UV-Visible), X-ray diffractometer, SEM, EDXs, and four-point probe. X-ray diffractometer results reported notable peaks with cubic polycrystalline phase. Desirable absorbance result and narrowed energy band gap upon addition of lower concentration (0.01mol%) of yttrium dopant were gotten from the optical result. The key elements of the fabricated thin materials were verified via the EDX spectra. More so, yttrium doping was seen to strongly influence the electrical parameters of CoSe thin materials via increased film thickness, resistivity, and decreased conductivity The fabricated thin materials have notable potential to be utilized in optical devices and solar cells.

1. Introduction

In recent times, a lot of attention has been bequeathed to Cobalt-based nanomaterials which are traceable to their fascinating physical features. They are befitting for use in modern devices like optoelectronic and photovoltaic devices (Agbo *et al.*, 2016). Chalcogenide thin film semiconductors are materials that comprise at least a chalcogen element like tellurium, sulfur, or selenium as an integral constituent (Obitte *et al.*, 2022). They possess excellent tuning characteristics, such as high transparency across the visible region and a major part of the infrared region of the spectrum. More so, they are viable for use in microelectronics, diodes, lasers, solar cells, transistors, imaging/sensor materials, optical filters, and photo-detectors (Agbo *et al.*, 2016; Obitte *et al.*, 2022; Akpu, *et al.*, 2021;

2022[a]; 2022[b]; Ikhioyaa, *et al.*, 2022; Osuwa *et al.*, 2012; Nwaokorongwu *et al.*, 2018) More so, there has been increasing interest in fabricating chalcogenide thin film semiconductors consisting due to their notable features of high optical absorption, good electrical conductivity, etc (Agbo *et al.*, 2016) and their need in making transistors, electronics and in the area of nanotechnology (Obitte *et al.*, 2022). In literature, thin-film semiconductors of various elemental selenides have been studied [(Agbo *et al.*, 2016; Obitte *et al.*, 2022; Akpu, *et al.*, 2021, 2022[a], 2022[b]; Ikhioyaa, *et al.*, 2022; Osuwa *et al.*, 2012, 2012; Chikwenze *et al.*, 2017). Cobalt Selenide (CoSe), as a binary metal chalcogenide is amidst the II-VI semiconductors with narrowed energy gap (Eg) of about 1.5 eV. They are of interest in research because they display a direct band-gap nature, as well as excellent optical, physical, chemical, luminescent, electronic, and quantum effects (Agbo *et al.*, 2016[a], 2016[b]) It has massive extensive and potential application possibilities in photo-catalysis, super-capacitor, and solar cells (Ikhioya *et al.*, 2020, Zhang *et al.*, 2019). They are also attractive because of the earth's abundance of Co. Cobalt selenides comprises two stable forms ($CoSe_2$, CoSe) and two viable compounds (Co_3Se_4, Co_2Se) at room temperature. A variety of methods such as CBD (Agbo *et al.*, 2016, Chikwenze *et al.*, 2017, Pramanik *et al.*, 1987; Govindasamy *et al.*, 2016), Electrodeposition (Ikhioya *et al.*, 2020; Zhang *et al.*, 2019); Liu *et al.*, 2010; Ikhioya *et al.*, 2023), Spray pyrolysis (Kima *et al.*, 2018), etc have been used to synthesize CoSe nano-materials.

Amidst these deposition techniques, the Spray pyrolysis method which is fast, inexpensive, and simple was employed in this study. It has been utilized in solar-cell fabrication and in the glass industry to grow conducting electrodes. More so, via this method, permeable and dense oxide thin materials, powders, and ceramic coatings can be fabricated. It has other noteworthy benefits, which include the capacity to alter the properties of the thin material by altering the structure of the preliminary material (incorporation of dopants and enhancement of the thin material micro-structure) and reduction of manufacturing cost when massive production is desired (Kima *et al.*, 2018; Dedova, 2007; George, 1992).

Agbo *et al.*, (2016) studied the influence of pH on the features of copper selenide thin materials synthesized via the CBD technique. The optical, morphological, and structural features of the thin materials were investigated. The X-ray diffraction analysis indicated that the thin materials are polycrystalline while the band-gap energy of the materials ranges between 2.80 eV to 3.10 eV. In their report, the result that showed that the properties of the films varied linearly with pH was obtained. Chikwenze *et al.*, (2017) investigated the optical and electrical features of CoSe thin materials. The samples were synthesized via a chemical bath with polyvinyl alcohol as a matrix agent to enhance the crystallite size and improve the energy band gaps before being annealed at 100 – 250 K. Optical measurements put band gaps between 4.25 – 4.30 eV. The ascertained wide band gaps place Copper selenide synthesized with CBD method as a potential material for power electronics devices. Liu et al. prepared CoSe thin materials onto tin oxide glass substrates via electrodeposition. The effect of potential variation during deposition was reported. CoSe thin material electro-deposited at a potential of -0.5V gave a suitable material for photovoltaic purposes based on the allowed direct interbank transition of 1.53 eV. Ikhioya *et al.*, (2023) also synthesized CoSe thin films doped with ytterbium through the electro-deposition method. The addition of ytterbium was observed to enhance the transmittance and narrowed the band gap energies of CoSe thin films making it serve as potential material for optical and photonic devices.

In this study, CoSe nanofilms were fabricated via spray pyrolysis technique and afterward doped with yttrium at different molar percentage concentrations. There is no published report on spray-fabricated yttrium-doped CoSe nanomaterials. The structural, composition, morphology, electrical, and optical features of the fabricated samples are reported alongside the doping influence on the primary compound in other to determine their feasible utilization in photovoltaic technology.

2. Experimental details: materials and method

The chemicals used for the spray pyrolysis fabrication of undoped and yttrium-doped Copper selenide nano films comprise Cobalt (II) acetate Tetrahydrate ($Co(NO_3)_2.6H_2O$), Selenium (IV) Oxide (SeO_2), yttrium (Y) and hydrogen chloride (HCl). The spray pyrolysis deposition technique is fundamentally a chemical growth method in which thin droplets of the supposed material are sprayed onto pre-heated substrates [18]. Soda-lime glass slides were used as substrate. Before deposition attention was paid to the cleaning and activation of these substrates using methanol, acetone, and deionized water. In an acetone solution, the substrates were ultrasonicated for 30 minutes later then rinsed in distilled H_2O and allowed to air dry.

2.1 Preparation of solutions

To prepare a 0.01mol of $Co(NO_3)_2.6H_2O$ solution, 1.455g/mol of it was dissolved in 500 ml of deionized H_2O. For 0.01mol of SeO_2 solution, 3.158g of it was dissolved with the aid of 5ml of HCl and an additional 100ml of deionized H_2O. Next, four 5ml yttrium (Y) solutions (which were used as a doping agent) were prepared for different concentrations selected as 0.01, 0.02, 0.03, and 0.04mol%.

2.2 Spray procedure/process

Cobalt selenide thin materials were grown onto the cleaned soda lime glass substrates at a constant substrate temperature of 400°C and atomizing voltage of 3.5KV (Fig. 1). Other parameters that were optimized during the procedure include; a flow rate of 0.07ml/min, a spray nozzle measuring 0.16mm for internal diameter and 0.32mm for external diameter, and a spray nozzle to substrate distance of 8mm. After growing CoSe the process was repeated by incorporating yttrium (Y) dopant at varying molarity as summarized in Table 1.

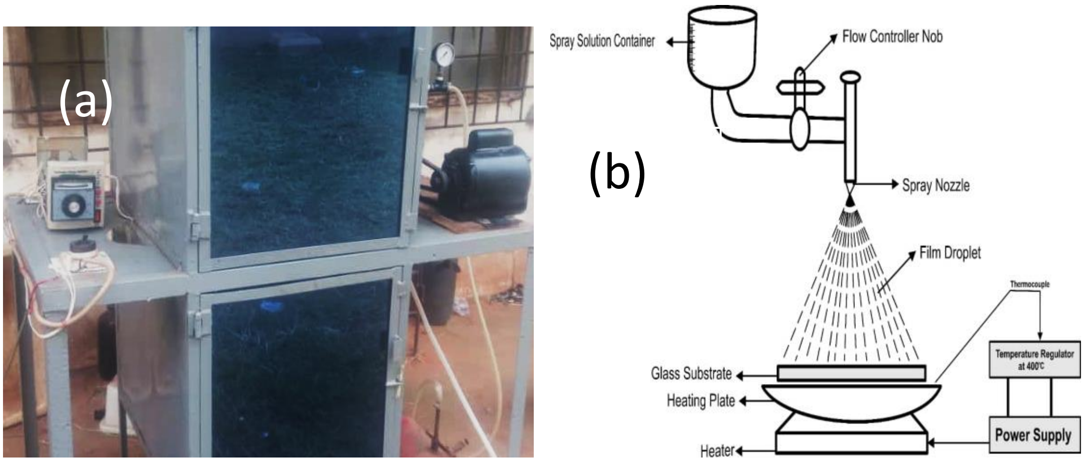

Fig. 1: (a) Pictural setup of spray pyrolysis and (b) Schematic diagram of spray pyrolysis

The fabricated thin materials were investigated with the aid of appropriate equipment and mathematical relations for an extensive examination of their optical features, structural, elemental composition content, and electrical properties. UV-Visible spectrophotometer model 756s was employed to ascertain the absorbance in the spectral wavelength regions of 300nm to 1100nm. The X-ray diffractometer model cu-kal (λ = 1.15418Â) was utilized for the structural analysis. This technique gives comprehensive information about the nature of crystal lattice, intensities of diffraction peaks, and crystallographic structure of natural and fabricated materials. The scanning electron microscopy model JEOL JSM 6360 was used to ascertain the morphology results while the EDXs technique was employed to ascertain the chemical constituent of the thin materials. Finally, the ancient-Jandel four-point probe technique was used to investigate the electrical features of the fabricated pure CoSe and yttrium-doped CoSe thin materials.

Table 1: Fabrication details of CoSe and CoSe:Y at varied dopant conc. (0.01 – 0.04 mol%)

Samples	Sample Code	$(Co(NO_3)_2.6H_2O)$ (mI)	SeO_2 (ml)	Yttrium (ml)	Dopant conc. (Yttrium) (mol%)
CoSe	CO	20	10		
0.01mol%Y;CoSe	COY (0.01mol%)	20	10	5	0.01
0.02mol%Y;CoSe	COY (0.02mol%)	20	10	5	0.02
0.03mol%Y;CoSe	COY (0.03mol%)	20	10	5	0.03
0.04mol%Y;CoSe	COY (0.04mol%)	20	10	5	0.04

3. Result and discussion

3.1. The results of the absorbance, reflectance, and transmittance of pure and yttrium-doped CoSe thin materials.

The spectrum plots of the absorbance values, transmittance values, and reflectance values of the fabricated samples at different dopant concentrations are presented in Fig. 2 (a-c). For absorbance result (Fig.2 (a)), all the deposited samples displayed a similar trend, elevated absorbance value in the UV which declines as the wavelength shifts toward the Vis-NIR region of the spectrum. The addition of a low percentage concentration of yttrium (0.01mol%) as a dopant was found to increase the absorbance of the CoSe thin films all through the electromagnetic region when compared to undoped CoSe. Further increase of the yttrium dopant (to 0.02, 0.03, and 0.04 mol%) drastically reduced the absorbance value even beyond the undoped CoSe absorbance value. As the dopant molar concentration increases, the thickness of the films also increases and the electromagnetic light radiation to the substrate decreases, which lowers the absorbance of the films at high doping. The high absorbance exhibited by CoSe doped with 0.01 mol% of yttrium in the UV range makes the material suitable for p-n junction formation in solar cells and photovoltaic purposes in general (Udofia *et al.*, 2017). The transmittance result for all the samples was deduced from the absorbance result using equation (1) (Ikhioyaa, *et al.*, 2021):

$$\mathbf{T} = \mathbf{10^{-A}} \quad (1)$$

The transmittance spectra plot of pure CoSe and yttrium doped CoSe thin film synthesized at varied dopant conc. is shown in Fig. 2 (b). All as-deposited samples displayed a similar trend, an increase in the percentage transmittance as the wavelength increased. The addition of a higher concentration of yttrium dopant (0.02, 0.03, and 0.04 mol%) was observed to tremendously improve the transmittance value of CoSe thin materials, especially in the visible - NIR range of the Spectrum, which amounts to its use as a good material for solar energy collector and optical devices (Liu *et al.*, 2010, Ikhioya *et al.*, 2019). Fig.2 (c) depicts the graphical result of the reflectance against wavelength for undoped and Y-doped CoSe thin material synthesized at varied dopant conc. (0.01, 0.02, 0.03, and 0.04 mol %). It is suggestive that both undoped and Y-CoSe are poorly reflective. A similar result was reported by Udofia and Okoli, 2017 in electrodeposited CuSe. The low reflectance exhibited by most of the materials makes them useful in anti-reflective coating (Agbo *et al.*, 2016) and potential material for solar control coatings (Udofia and Okoli, 2017)

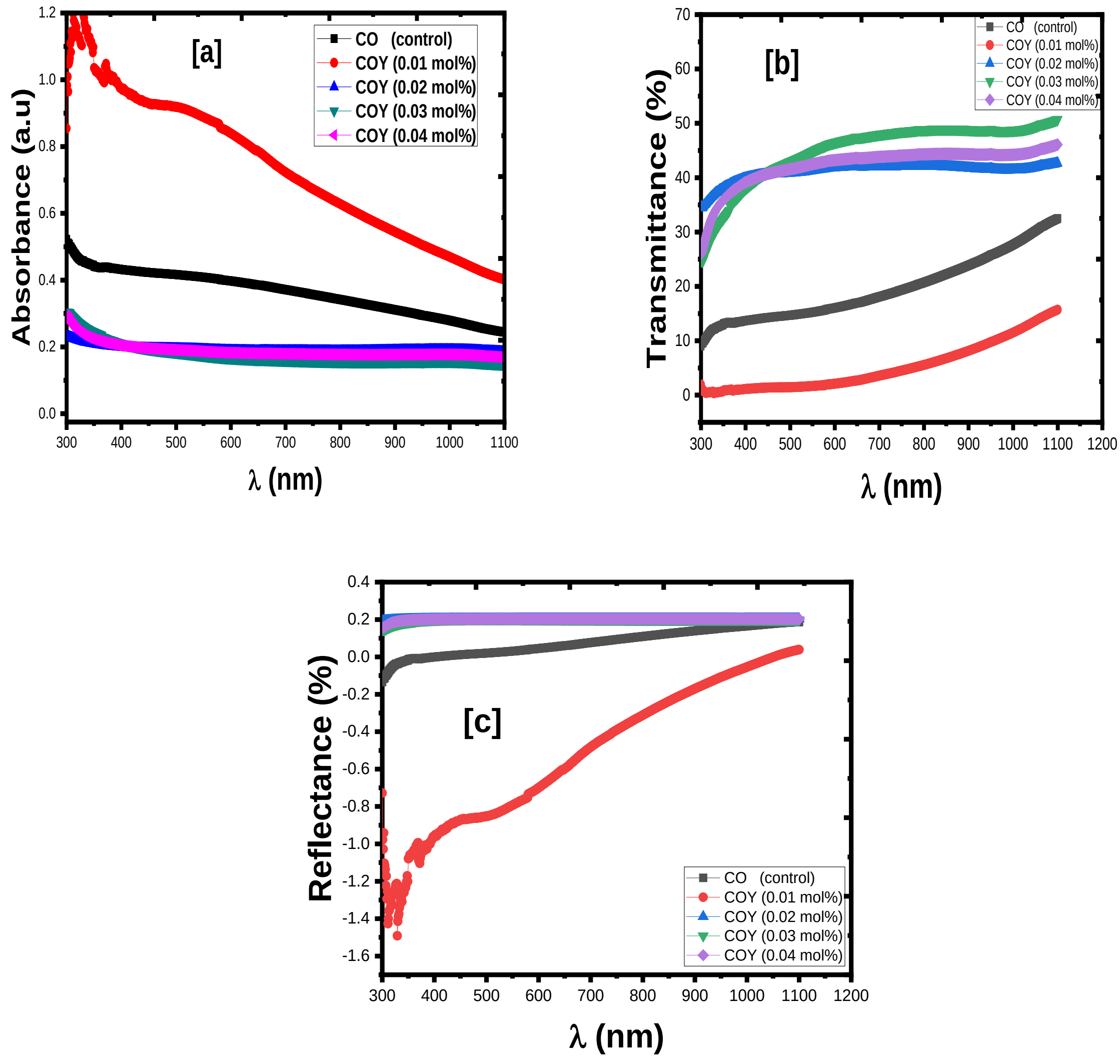

Fig. 2: Absorbance graph [a] transmittance graph [b] and reflectance graph [c] of CoSe and yttrium doped CoSe at varied dopant concentrations.

Fig. 3 (a-d) reveals the graph of absorption coefficient (α), energy band gap (E_g), refractive index (n), and extinction coefficient (k) to hν for pure and yttrium-doped CoSe thin material synthesized at varied dopant conc. (0.01 mol%, 0.02 mol%, 0.03 mol% and 0.04 mol%). The absorption coefficient (α) was evaluated out of the transmittance and material thickness using equation (2) (Ikhioya *et al.*, 2021):

$$\propto = \frac{1}{d} \ln \left(\frac{1}{T}\right) \quad (2)$$

Fig 3 (a) depicts the absorption coefficient result which is the level of incident light penetration before absorption. The reveals increase with a rise in photon energy for undoped and Y-CoSe at 0.01mol%, while the other CoSe samples doped with 0.02, 0.03, and 0.04mol% of yttrium, had almost a constant value all through the photon energy axis irrespective of the increase in dopant concentration. The energy band gap (Eg) of pure CoSe and yttrium doped CoSe at varied dopant conc. was deduced via equation (3) (Onwuemeka *et al.*, 2018)

$$(\propto \mathbf{hv})^2 = \mathbf{A}(\mathbf{hv} - \mathbf{E_g}) \quad (3)$$

Fig. 3 (b) shows a graph of $(\alpha hv)^2$ against hv for pure CoSe and yttrium-doped CoSe at varied dopant concentrations. From this graph (Fig. 2(b)), the energy band gap of the materials was evaluated by extrapolating the straight area of the graph down to the hv axis at $(\alpha hv)^2 = 0$. The undoped CoSe had an energy band gap value of 1.50 eV while the yttrium doped CoSe at 0.01, 0.02, 0.03 and 0.04 mol% recorded 1.25 eV, 1.81 eV, 1.75 eV, and 1.60 eV respectively. The values clearly show that the incorporation of yttrium dopant increases the energy gap except for CoSe doped with 0.01 mol% of Yttrium. The energy band gap values attained in this study are in line with the report by (Liu *et al.*, 2010) for electrodeposited CoSe thin films. The band gap value suggests that CoSe and CoSe doped with a low concentration of yttrium is a very good potential material for fabricating thin film solar cells (Ikhioya *et al.*, 2020, 2021). The refractive index result was evaluated from the reflectance values using equation (4) (Ikhioya *et al.*, 2021: Lim *et al.*, 2020)

$$\mathbf{n} = \frac{1+\sqrt{\mathbf{R}}}{1+\sqrt{\mathbf{R}}} \quad (4)$$

Fig 3 (c) displays the graphical result of refractive index versus photon energy for pure CoSe and yttrium-doped CoSe at varied dopant concentrations. It was observed that CoSe doped with 0.01 mol% of yttrium increases with a rise in photon energy and displays the maximum refractive index value of 7.10 at 2.0 eV, undoped CoSe decreases with an increase in photon energy with the maximum value of 6.5 at 0.6 eV, the other CoSe samples doped with 0.02, 0.03 and 0.04 mol% of yttrium had almost a constant value of 2.7 all through the photon energy axis. The absorption coefficient gives information on the extinction coefficient (Sreedevi *et al.*, 2015) and is related thus; to equation (5) (Agbo and Nwofe, 2015);

$$\mathrm{K} = \frac{\propto\lambda}{4\pi} \quad (5)$$

Figure 3 (d) displays the graphical results of the extinction coefficient against photon energy for undoped and Y-CoSe thin film synthesized at varied dopant conc. (0.01 mol%, 0.02 mol%, 0.03mol% and 0.04 mol %). The undoped and Y-CoSe at 0.01 mol% was observed to increase with a rise in photon energy before decreasing gradually while the other CoSe samples doped with 0.02, 0.03, and extinction coefficient value in the UV region and minimum values in the IR region which is a captivating property for photonic devices (Ikhioya *et al.*, 2020). 0.04 mol% of yttrium had almost a constant value all through the photon energy axis irrespective of the increase in dopant concentration. This infers that the synthesized films recorded a maximum.

The dielectric constant, [Ɛ = Ɛr + Ɛi] can be defined as a basic inherent feature of the material. It has two parts; the real and the imaginary part which can be expressed in terms of refractive index and extinction coefficient as seen in equations (6) and (7) respectively (Ikhioya *et al.*, 2021):

$$\varepsilon_r = \mathbf{n}^2 + \mathbf{k}^2 \quad (6)$$

$$\varepsilon_i = \mathbf{2nk} \quad (7)$$

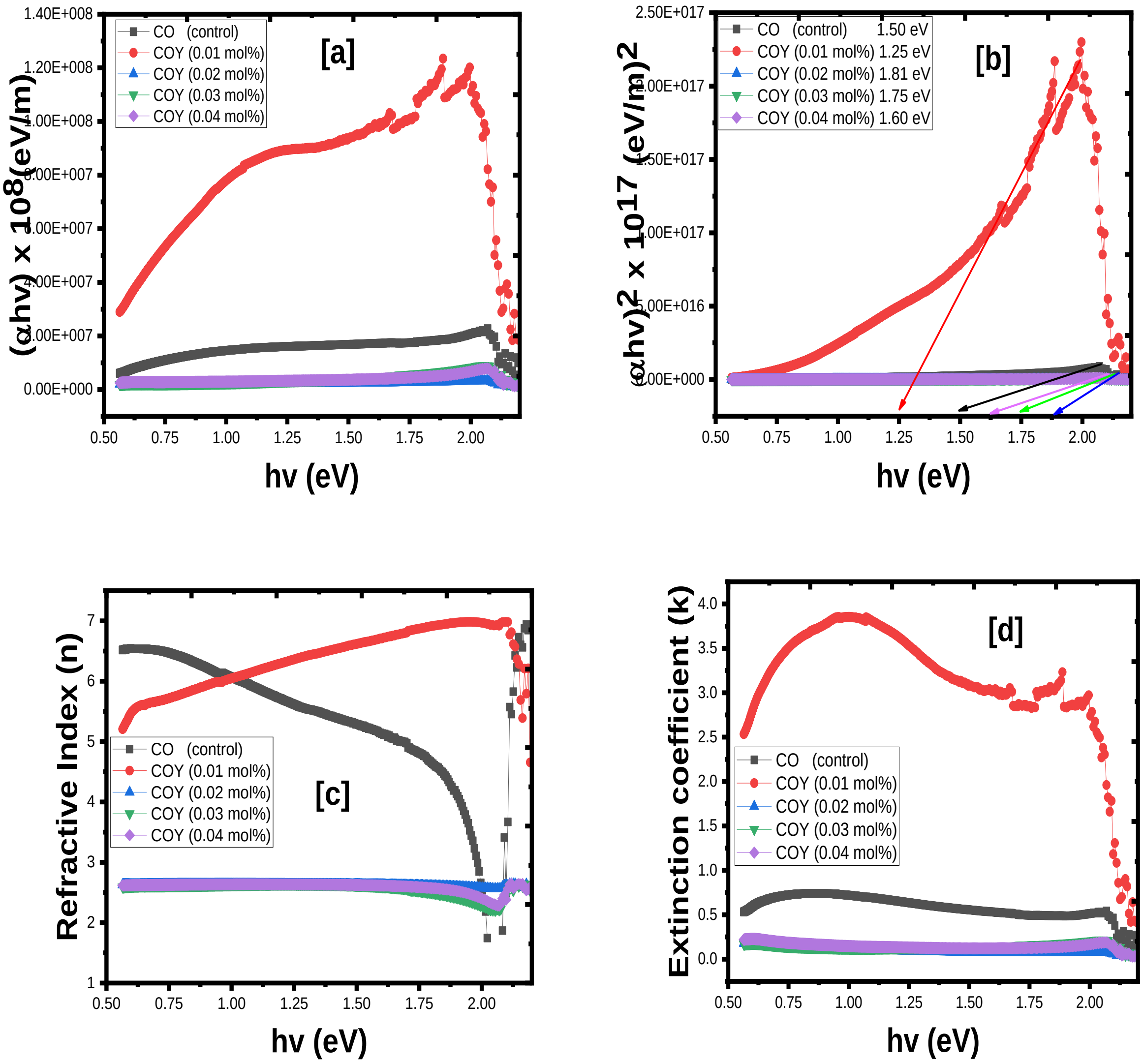

Fig. 3: Graph of (a) Absorption coefficient (b) $(\alpha h\nu)^2$ (c) refractive index (d) Extinction coefficient to $h\nu$ for pure and yttrium-doped CoSe at varied dopant conc.

In this study, the incorporation of yttrium-dopant on CoSe heightened both its real and imaginary dielectric constant values as seen in Fig. 4 (a) and Fig. 4 (b) respectively. This reveals that doped Y-CoSe films can be used for the commercial manufacturing of solar cells and quality solar panels. While the real part is observed to be almost constant as the photon energy increases, the imaginary part is seen to decline gradually. A ditto trend in the real dielectric part was also reported by (Ikhioya *et al.*, 2020). in electrodeposited CoSe doped with ytterbium. More so, a similar imaginary dielectric constant result was recorded by (Jeroh, 2018) in an electrostatic sprayed Eu-doped CdSe. The optical conductivity, (σ_{opt}) is the optical response of a transparent solid and it can be calculated using equation (8) (Lim *et al.*, 2020):

$$\sigma opt. = \frac{\alpha n c}{4\pi} \quad (8)$$

The graph of optical conductivity for CoSe and yttrium-doped CoSe at varied dopant concentrations is shown in Fig. 4 (c). All as-deposited samples showed a similar trend of a slight increase in optical conductivity value as the photon energy increases apart from CoSe doped with

0.01mol% of yttrium which decreases with a rise in photon energy. The undoped CoSe displayed the maximum optical conductivity value among the other thin materials. More so, the addition of a high concentration of yttrium dopant was seen to reduce the optical conductivity of pure CoSe

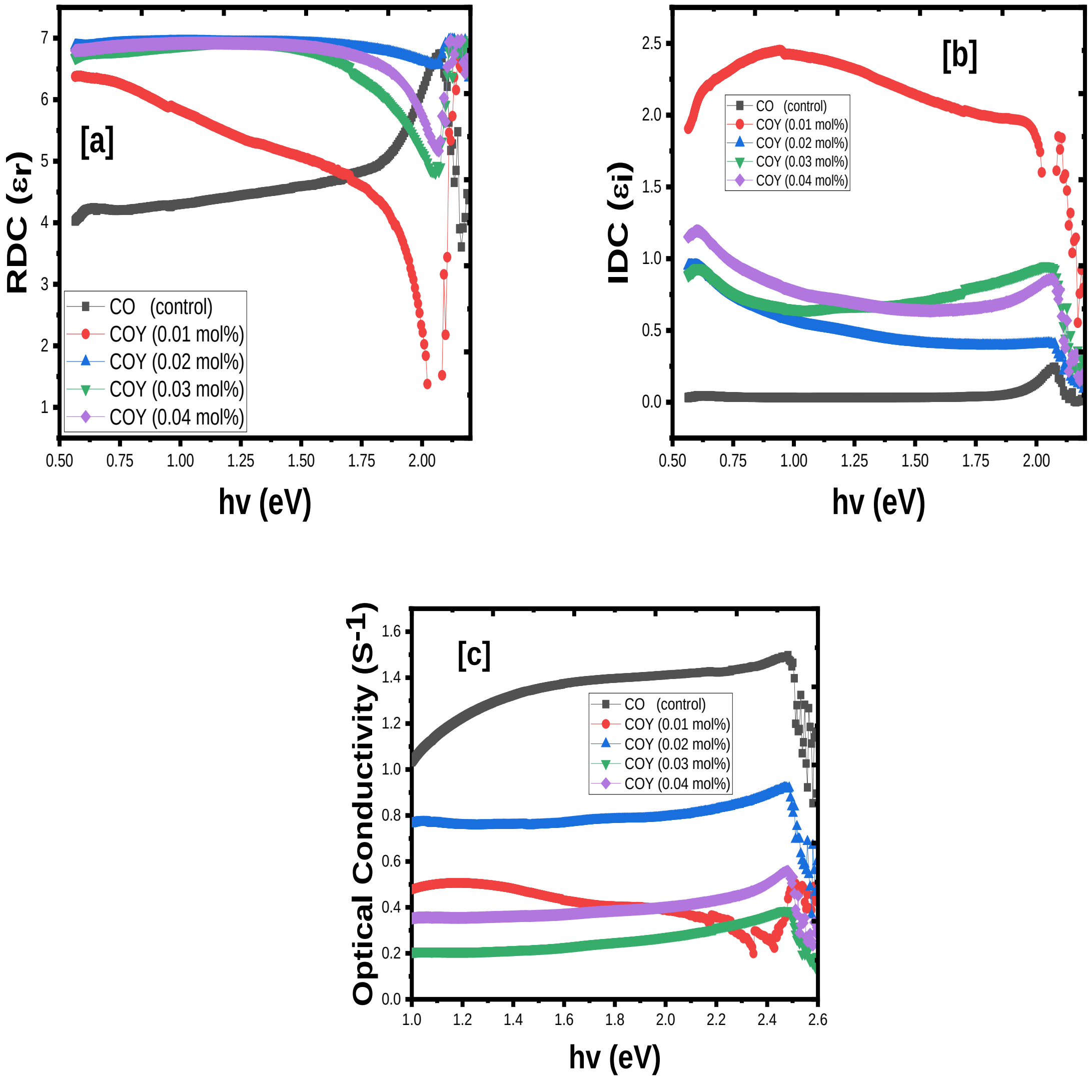

Fig. 4: (a) Real dielectric const. (b) imaginary dielectric const. and (c) optical Conductivity to hv for pure and yttrium-doped CoSe at varied dopant conc.

3.2. X-ray diffraction results

Fig. 5 reveals the X-ray diffraction pattern of undoped and yttrium-doped CoSe thin materials synthesized at varied yttrium mol% concentrations. The pattern reveals a cubic polycrystalline structure for both undoped and Y-doped CoSe films. Our findings correspond with the result reported by (Agbo *et al.*, 2016) for CoSe deposited via the chemical bath technique. Peaks corresponding to (111), (200), (210), (211), (300) and (311) were obtained in the XRD analysis. The introduction of a high concentration of yttrium dopant (0.02 to 0.04mol%) on CoSe films enhanced the crystallinity as seen from the clearly defined increased peak intensity. (Ikhioya *et al.*, 2020) also reported improved crystallinity of CoSe when doped with ytterbium. The information obtained during the XRD analysis was used to calculate some structural parameters like crystalline size (D), dislocation density, etc (Ikhioya *et al.*, 2020) as outlined in Table 2. Evaluation of the structural properties in Table 2 was estimated for the ave. crystallite size, D utilizing Scherer's mathematical relation, d-spacing, d, lattice constant, a, and dislocation density, δ using equations (9-12) (Osuwa *et al.*, 2012; Ikhioya *et al.*, 2020; Okereke and Ekpunobi, 2011):

$$D = {}^{k\lambda}/_{\beta\cos\theta} \quad (9)$$

$$d = {}^{\lambda}/_{2\sin\theta} \quad (10)$$

$$a = d\sqrt{h^2 + k^2 + l^2} \quad (11)$$

$$\delta = {}^{1}/_{D} \quad (12)$$

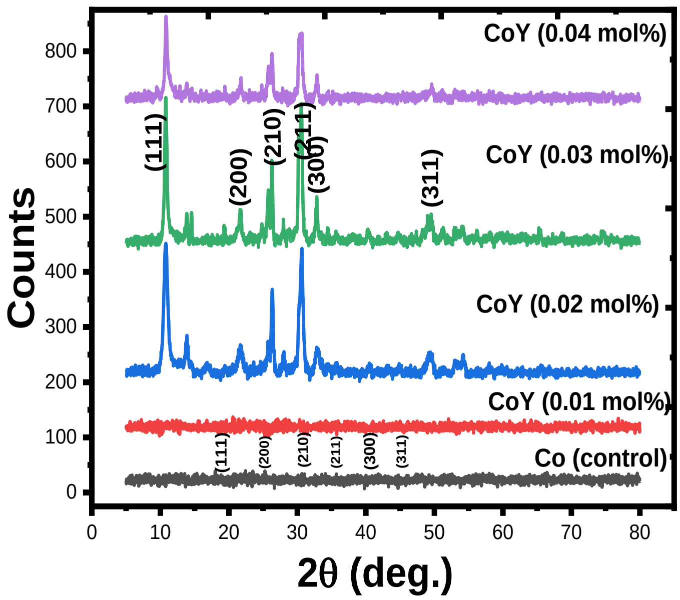

Fig. 5: X-Ray Diffraction pattern of CoSe and yttrium-doped CoSe at varied molar percent dopant concentrations

Table 2: Some structural information for CoSe and Y:CoSe at varied mol% dopant conc.

Material	2θ (deg.)	d (Å)	a (Å)	β	hkl	D (nm)	Δ (m^2)
CO	18.3126	4.8401	8.3833	0.1851	111	0.7584	5.2707
COY (0.01 mol%)	11.1759	7.9097	13.700	0.1847	200	0.7523	5.3564
COY (0.02 mol%)	21.5035	4.1285	8.2571	0.2092	210	0.6734	6.6970
COY (0.03 mol%)	26.4786	3.3630	6.7261	0.1477	211	0.9624	3.2793
COY (0.04 mol%)	30.8703	2.8938	6.4709	0.2244	300	0.6369	7.4175

3.3 Morphology and elemental results

The SEM imaging as seen in Fig 6 (a-e) reveals the morphologies and microstructural details of undoped CoSe and Y-doped CoSe (0.01 mol% to 0.04 mol%). SEM image, as shown in Figure 6 (a) revealed that the undoped CoSe thin materials were very rough containing randomly oriented non-uniform thin particles. The addition of a low concentration of Y dopant (0.01 mol%) as seen in Fig. 6 (b-d) improved the morphology with some agglomerations while Fig. 6 (e) which is CoSe doped with 0.04 mol% of Y shows a homogenous distribution of compact rectangular-like nanograins.

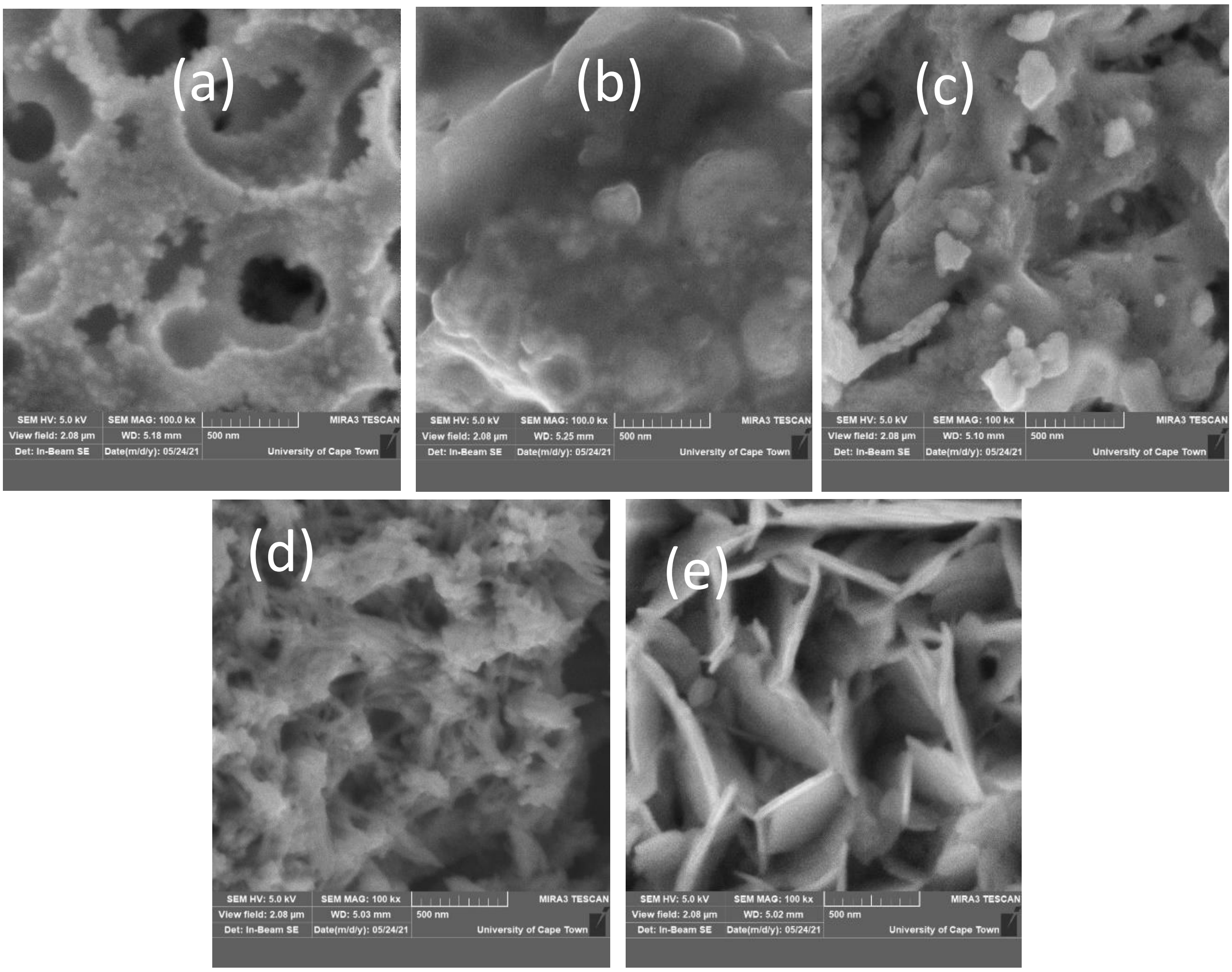

Fig.6: Pictorial SEM microstructure of (a) pure CoSe; Y-doped CoSe (b) 0.01 mol%, (c) 0.02 mol%, (d) 0.03 mol%, and (e) 0.04 mol%).

The densely packed grains could be due to an increase in the dopant concentration. The dopant was seen to significantly alter the morphology of the undoped sample. The elemental compositions of the as-deposited thin materials are shown in Fig. 7 (a-c) and Table 3. Apart from S, C, and O which are confirmed to be the elemental composition of the substrate, the other elements present are Co, Se, and Y whose counts are far way above other elements. This confirms that the deposited materials are CoSe and Y-doped CoSe thin materials as seen in Fig. 7 (a) and Fig. 7 (b-e) respectively.

3.4 Electrical results

The thickness, t of the thin materials was determined with the aid of a thickness probe while the sheet resistance, resistivity, and conductivity of the samples were estimated using the following relations (13-15) respectively [31]:

$$\mathbf{R_s = R\left({}^{V}/_{I}\right)} \qquad 13$$

Where K = $\pi/_{ln2}$

$$\boldsymbol{\rho = t \times R_s} \qquad 14$$

$$\boldsymbol{\sigma = {}^{1}/_{\rho}} \qquad 15$$

where R_s is the sheet resistance, , R is the resistance, V is the voltage, I is the current, K is a constant, $\boldsymbol{\rho}$ is the resistivity, and $\boldsymbol{\sigma}$ is the conductivity.

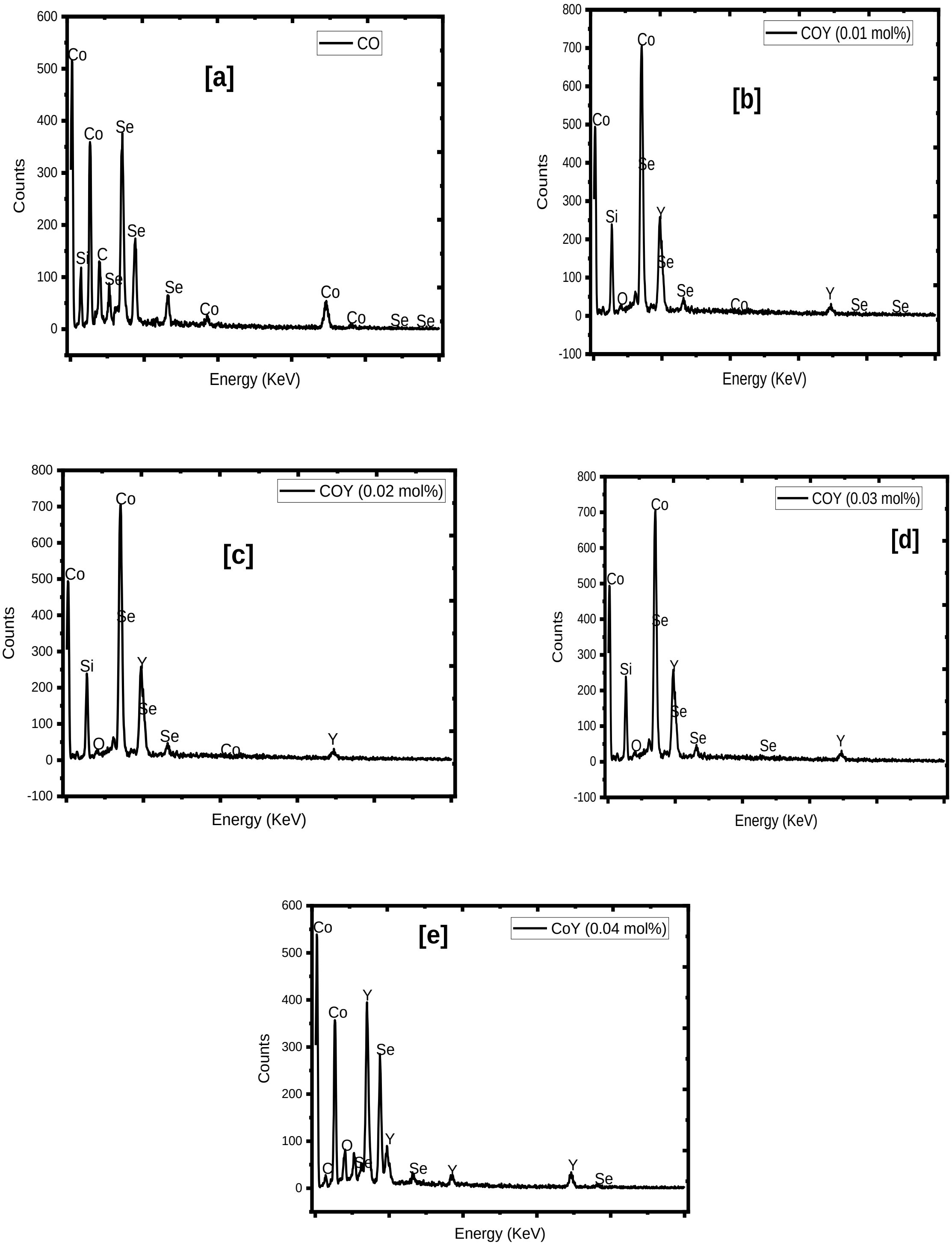

Fig 7: EDXs plot of (a) pure CoSe (b) 0.01 mol%, (c) 0.02 mol%, (d) 0.03 mol%, and (c) 0.04 mol% Y-doped CoSe thin film materials

The film thickness and electrical features of CoSe and yttrium incorporated CoSe (at varied dopant conc.) thin materials are summarized in Table 4 which shows that the incorporation of yttrium in the CoSe tin material greatly altered the electrical features and the thin material thickness. Just as the yttrium conc. in pure CoSe increases from 0 to 0.04 mol%, there was also an increase in the thin material's resistivity with an increasing material thickness of 135.15 nm to 159.10 nm and a decline in conductivity. Figure 8 depicts the connection between resistivity and conductivity with material thickness. As the film's thickness increases, the material's electrical conductivity declines in tandem with an increase in its resistivity. The yttrium dopant has an impact on the synthesized films, increasing the thickness, and resistivity, and lowering the electrical conductivity of the films as the dopant concentration increases. It is an excellent material for the fabrication of solar cells due to the high conductivity of pure CoSe and yttrium-doped CoSe thin films (Osuwa *et al*., 2012).

Table 3: Outline of the atomic weight of basic elements in EDXs

CoSe [a]		**Y-doped CoSe 0.01 mol% [b]**		**Y-doped CoSe 0.02 mol% [c]**		**Y-doped CoSe 0.03 mol% [d]**		**Y-doped CoSe 0.04 mol% [e]**	
Elements	Atomic Weight (%)	Elements	Atomic Weight (%)	Elements	Atomic Weight (%)	Elements	Atomic Weight (%)	Elements	Atomic Weight (%)
Cobalt	60.80	Cobalt	60.79	Cobalt	60.79	Cobalt	60.79	Cobalt	60.47
Selenium	33.13	Selenium	23.13	Selenium	23.13	Selenium	22.12	Selenium	16.02
Carbon	3.63	Silicon	5.67	Silicon	5.64	Silicon	5.64	Carbon	1.40
Silicon	2.44	Oxygen	1.40	Oxygen	1.40	Oxygen	1.40	Yttrium	19.09
-	-	Yttrium	9.01	Yttrium	9.04	Yttrium	10.05	Oxygen	3.02

Table 4: Electrical features of CoSe and yttrium-doped CoSe at varied dopant conc.

Samples	**Material Thickness in nm**	**Resistivity, X 10^{-6} in Ω.m**	**Conductivity, X 10^{-5} S/m**
CO	132.15	5.920	1.689
COY (0.01mol%)	143.18	5.996	1.667
COY (0.02mol%)	144.12	6.297	1.588
COY (0.03mol%)	151.14	6.432	1.554
COY (0.04mol%)	159.10	6.660	1.501

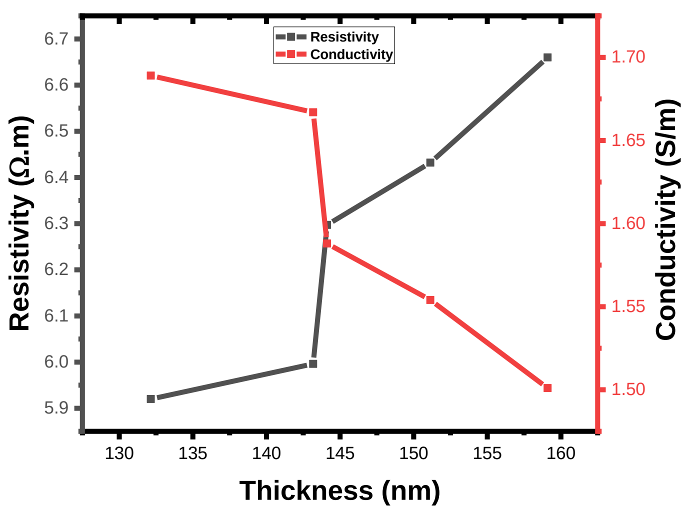

Fig. 8: The plot of conductivity and resistivity of pure and yttrium doped CoSe (at varied dopant concentrations) with material thickness.

Conclusion

Cobalt selenide and yttrium doped cobalt (Y:CoSe) thin materials have been satisfyingly fabricated by spray pyrolysis technique on a soda-lime substrate. The films were deposited at constant temperatures and varying dopant concentrations (0.01, 0.02, 0.03, and 0.04 mol %). The fabricated thin materials were evaluated to understand their optical, structural, morphological, elemental composition, and electrical features. The impact of yttrium doping on the aforementioned features of CoSe is reported in this research work. For the undoped and Y-doped CoSe, the optical analysis gave moderate (> 50%) transmittance with energy bandgaps stretching from 1.25 eV to 1.81 eV. The addition of yttrium as a dopant to pure CoSe films was seen to improve the optical features and the electrical studies reveal that the films are semiconducting materials. The XRD result revealed a polycrystalline cubic structure and the addition of a higher concentration of yttrium dopant on the films enhanced the crystallinity as revealed in the increased peak intensity. The presence of the key elements; cobalt, selenium, and yttrium were reaffirmed from the EDXs result. Yttrium doping was seen to strongly influence the electrical parameters of CoSe thin materials via increased film thickness, resistivity, and decreased conductivity. The high absorbance exhibited by CoSe doped with 0.01 mol% of yttrium in the UV range makes the material suitable for p-n junction formation in solar cells and photovoltaic purposes in general. The Y:CoSe is a very promising semiconductor as it could be beneficial in the fabrication of photonics, optical devices, and optoelectronics due to its remarkable optical, structural as well as electrical properties.

Declarations

Ethical Statement: The writers' research and findings are presented in full and precise detail in the paper.
Conflicts of Interest: There are no known conflicts of interest.
Author Contribution: Nwamaka I. Akpu, Imosobomeh L. Ikhioya, Emmanuel O. Okechukwu: conceptualization, methodology, graphical plots. Nwamaka I. Akpu, Imosobomeh L. Ikhioya, Cissan A. Sylvanus, Elizabeth C. Nwaokorongwua, Leticia U. Okoli wrote the original draft, data analysis, editing, proofreading, and manuscript handling. Azubuike J. Ekpunobi and Imosobomeh L. Ikhioya: supervision, initial corrections, and suggestions. All the authors read and approved the final manuscript.
Funding: For this study, the authors were not given any funding.
Data Availability Statement: The data supporting the study's conclusions are available upon request from the corresponding author.

References

Agbo P. E and Nwofe P. A. (2015) Comprehensive Studies on the Optical Properties of ZnO-Core Shell Thin Films. *Journal of Nano. Adv. Mat.* 3, 2, 63-97.

Agbo P. E., Nwofe A.P., Elekwa C.A., Nnabuchi N.M, (2016) Comparative Study of the Optical Properties of CdZnS Deposited by Two methods. *Journal of Ovonic Research*, 12(3) 163 - 169

Agbo P.E., Nwofe P.A., Chikwenze R.A and Famuyibo R.A (2016) Effect of pH on Properties of CoSe Thin Films Deposited by Chemical Bath Technique, *African Journal of Basic & Applied Sciences* 8 (3) 152-156, DOI: 10.5829/idosi.ajbas.2016.8.3.22836

Akpu N. I., et al., (2021) Investigation On The Influence of Varying Substrate Temperature On The Physical Features of Yttrium Doped Cadmium Selenide Thin Films Materials, *SSRG International Journal of Applied Physics* 8 (2), 37-46, doi:10.14445/23500301/ IJAP-V8I2P106

Akpu N.I et al., (2021) Influence of Substrate Temperature on the Photovoltaic/ Optoelectronic properties of Spray Synthesized Yttrium Copper Selenide(YCS) Thin Films. Arabian Journal for Science and Engineering https://doi.org/10.1007/s13369-021-06455-0

Akpu N.I., et al., (2022) Synthesis and characterization of novel yttrium- incorporated copper selenide (CuSe:Y) thin materials for solar energy applications. *Mater. Sci: Mater. Electron* 33, 1154–116, https://doi.org/10.1007/s10854-021-07397-x

Chikwenze R. A., Uba J. I., Arikpo J. U., (2017) Optical and electrical properties of chemical bath deposited cobalt selenide thin film. *Chalcogenide Letters* 14 (6) 211 – 216.
Dedova T., (2007) Chemical spray pyrolysis deposition of zinc sulfide thin films and zinc oxide nanostructured layers. Doctoral dissertation Tallinn University of Technology, Estonia.
George J., Preparation of Thin Films; CRC Press: New York, (1992) 339-342.
Govindasamy G., Murugasen, S. Sagadevan (2016) Optical and Electrical Properties of Chemical Bath Deposited Cobalt Sulphide Thin Films. *Materials Research*. DOI: http://dx.doi.org/10.1590/1980-5373-MR-2016-0441
Ikhioya I. L., Nwamaka I. A, Edwin U. O, Samson O. A, Ishaq A, Maaza M. & Fabian I. E. (2023) Enhanced physical properties of nickel telluride metal chalcogenide material with molybdenum dopant, *Materials Research Innovations*, *https*://doi.org/10.1080/14328917.2023.2222465
Ikhioya I. L., Okoli D. N., Ekpunobi A. J. (2019) Effect of Temperature on SnZnSe Semiconductor Thin Films for PhotovoltaicApplication. *SRG International Journal of Applied Physics (SSRG-IJAP)*, 6, 55 - 67
Ikhioya I. L., Whyte G. M., Nkele A. C. (2023) Temperature-modulated nanostructures of ytterbium-doped Cobalt Selenide (Yb-CoSe) for photovoltaic applications. *Journal of the Indian Chemical Society* 100, 100848, https://doi.org/10.1016/j.jics.2022.100848
Ikhioya I.L et al., (2020) A study on the effects of varying concentrations on the properties of ytterbium-doped cobalt selenide thin films. *Optical Materials* 101 10973, https://doi.org/10.1016/j.optmat.2020.109731
Ikhioya I.L, Akpu N.I and Nkele A.C (2021) influence of ytterbium (Yb) dopant on the optical properties of electrochemically deposited zinc oxide (ZnO) films. *Mater. Res. Express*, 6, 016403, https://doi.org/10.1088/2053-1591/abd5d6
Ikhioyaa I.L., et al., (2022) Influence of temperature on energy band gap and other properties of undoped and cadmium doped manganese sulphide (MnS:Cd) synthesized for photovoltaic and optoelectronic. *Asian Journal of Nanoscience and Materials* 5, 88-97, DOI: 10.26655/AJNANOMAT.2022.2.1
Jeroh M.D., Ekpunobi A.J., Okoli D.N. (2018) Optical analytical studies of Electrostatic sprayed Eu-doped Cadmium selenide nanofilms at different temperatures. *Journal of Nano and Electronic Physics*, 10(3)
Koo K. J., Jong H.K, Yun C. K. (2018) Electrochemical properties of multicomponent oxide and selenide microspheres containing Co and Mo components with several tens of vacant nano rooms synthesized by spray pyrolysis. *Chemical Engineering Journal* 333, 665-677. doi.org/10.1016/j.cej.2017.09.169
Lim H. C., Park E., Shin I. S., Hong J. I. (2020) Electrodeposition of zinc oxide nanowires as a counter electrode in electrochromic devices, *Bull. Korean Chem. Soc.* 41, 358–61
Liu F., Wang B., Lai Y., Li J, Zhang Z., Liu Y., (2010). Electrodeposition of Cobalt Selenide Thin Films. *Journal of The Electrochemical Society*, 157 (10), D523-D527
Nandiyanto A.B.D., Risti Ragadhita H. N. P., Suryatno Wiganepdo Soegoto S. W. (2022) Cost Analysis and Economic Evaluation for TiO2 Synthesis using Sol-Gel Method, *Mor. J. Chem.* 10 N°1, 013-021
Nwaokorongwu E.C. et al., (2018) Growth and Optical Characterization of Copper Sulphide Thin Films by Sol-Gel Technique. *Int. J. Inno. Scientific & Eng. Tech. Res.* 6 (2), 38-44.
Obitte B.C.N., Ikhioya I.L., Whyte G.M., Chime U.K., Ezekoye B.A., Ekwealor A.B.C., Maaza M., Fabian I. E, (2022) The effects of doping and temperature on properties of electrochemically deposited Er^{3+} doped ZnSe thin films, *Optical Materials 124* 111970. https://doi.org/10.1016/j.optmat.2022.111979
Okereke N.A., Ekpunobi A.J. (2011) XRD and UV-VIS-IR Studies of Chemically-synthesized Copper Selenide Thin Films. *Research Journal of Chemical Sciences*, 1(6), 64-70,
Onwuemeka J.I, Ekpunobi A.J. (2018) Synthesis of CdO:SnO2 alloyed thin films for solar energy conversion and optoelectronic applications, *J. Mater. Sci.: Mater. Electron.* 29, 9176–83
Osuwa J. C., Chigbo N. I. (2012) Characterization of structural and electrical properties of electro-deposited cadmium telluride (CdTe) thin films at varying deposition time on glass FTO. *Chalcogenide Letters*, 9 (12) 501 – 508.
Osuwa J. C., Chigbo N. I., Oriaku C. I. (2012) Effects of temporal variations in deposition on the optical and solid state properties of electro-deposited cadmium telluride (CdTe) thin films on glass FTO. *Chalcogenide Letters* 9 (1), 447 – 455.
Osuwa J.C., Osuji N.U, (2011) Analysis of electrical and micro-structural properties of annealed antimony sulphide (Sb2S3) thin films. *Chalcogenide Letters* 8(9), 571 –577
Pramanik P., Battacharya S and Banu, P.R. (1987) A solution growth technique for the deposition of cobalt selenide thin film. *Thin Solid Films*, 149, L81-L84.

Sreedevi G., Vasudeva R. M., Chinho P, Jeon C.W. and Ramakrishna R. K. (2015) Comprehensive Optical Studies on SnS Layers Synthesized by Chemical Bath Deposition. *Optical Materials* 42, 468–475

Udofia K. I and Okoli D.N (2017) investigation of the optical, structural and surface morphology properties of Copper selenide thin film. International journal of scientific research and education. 5, 4, 6357-6363

Yadav A. A (2014) Nanocrystalline copper selenide thin films by chemical spray pyrolysis, *J. Mater. Sci. Mater. El.* 25, 1251–1257, DOI 10.1007/s10854-014-1717-5

Zhang X., Jiangfeng G, Kaixiao Z, Weihua Z, Jing-C L , and Qingping D (2019) All-Solid-State Asymmetric Super capacitor Based on Porous Cobalt Selenide Thin Films. *Journal of alloys and compounds.* 772, 25 – 32.

(2023) ; http://www.jmaterenvironsci.com